

GDEPO: Group Dual-dynamic and Equal-right Advantage Policy Optimization with Enhanced Training Data Utilization for Sample-Constrained Reinforcement Learning

Zhengqing Yan¹, Xinyang Liu¹, Yi Zhang¹, Fan Guo¹, ChengXun Jia¹, Junchen Wan¹, Yao Liu¹, Qi Liu¹, Jihao Huang¹, Kang Song¹

Abstract—Automated Theorem Proving (ATP) represents a fundamental challenge in Artificial Intelligence (AI), requiring the construction of machine-verifiable proofs in formal languages such as Lean to evaluate AI reasoning capabilities. Reinforcement Learning (RL), particularly the high-performance Group Relative Policy Optimization (GRPO) algorithm, has emerged as a mainstream approach for this task. However, in ATP scenarios, GRPO faces two critical issues: when composite rewards are used, its relative advantage estimation may conflict with the binary feedback from the formal verifier; meanwhile, its static sampling strategy may discard entire batches of data if no valid proof is found, resulting in zero contribution to model updates and significant data waste. To address these limitations, we propose Group Dual-dynamic and Equal-right Advantage Policy Optimization (GDEPO), a method incorporating three core mechanisms: 1) dynamic additional sampling, which resamples invalid batches until a valid proof is discovered; 2) equal-right advantage, decoupling the sign of the advantage function (based on correctness) from its magnitude (modulated by auxiliary rewards) to ensure stable and correct policy updates; and 3) dynamic additional iterations, applying extra gradient steps to initially failed but eventually successful samples to accelerate learning on challenging cases. Experiments conducted on three datasets of varying difficulty (MinF2F-test, MathOlympiadBench, PutnamBench) confirm the effectiveness of GDEPO, while ablation studies validate the necessity of its synergistic components. The proposed method enhances data utilization and optimization efficiency, offering a novel training paradigm for ATP.

Index Terms—automated theorem proving, large language models, reinforcement learning, advantage function, formal verification.

I. INTRODUCTION

THE rapid advancement of Large Language Models (LLMs) has opened new avenues for applying Artificial Intelligence (AI) to formal reasoning. Automated Theorem Proving (ATP), a core challenge in AI, requires systems to construct machine-verifiable mathematical proofs in formal languages such as Lean [1]–[3]. Recent progress in ATP on complex theorem-proving tasks stems from the strong prior knowledge and generative capabilities of LLMs, coupled with the

availability of extensive training and validation datasets [4]–[9]. Notably, AlphaGeometry [10] has demonstrated problem-solving performance approaching International Mathematical Olympiad (IMO) medalist levels, signaling a transition of LLM-driven ATP from theoretical exploration toward practical deployment.

A prevailing approach integrates LLMs with Reinforcement Learning (RL) algorithms, leveraging precise feedback from formal verifiers to guide policy optimization. Among these, Group Relative Policy Optimization (GRPO) [11] has gained widespread adoption due to its strong empirical performance. However, GRPO faces three critical limitations in the ATP setting. First, when composite rewards are used, its advantage computation may assign negative advantages to correct trajectories due to interference from other reward components—a mathematical possibility formally detailed in Section VI. To avoid this issue, many works resort to a single binary correctness reward, which forfeits RL’s essential role in aligning LLM outputs with human preferences. Second, data efficiency is poor: under a single binary reward, groups containing only incorrect trajectories yield zero advantages across all samples, leading to the discarding of entire batches despite potentially informative partial reasoning—particularly problematic when challenging samples dominate the training set. Third, a fixed number of optimization iterations treats all samples uniformly, ignoring their varying learning potential.

To address the aforementioned issues, we propose the Group Dual-dynamic and Equal-right Advantage Policy Optimization (GDEPO) method, whose workflow is illustrated in Fig.1. This approach identifies and discards ineffective training data, then re-explores valid solutions. It ensures correct optimization direction under arbitrary reward weight combinations through the equal-right advantage mechanism. Furthermore, for initially invalid training instances that yield correct proofs after re-exploration, the method applies a dynamic number of additional backward passes to rapidly assimilate knowledge that is challenging yet solvable for the model.

We first validate the effectiveness of GDEPO on three benchmarks of varying difficulty: MinF2F-test, MathOlympiadBench, and PutnamBench. Ablation studies further confirm the necessity of each component and their synergistic interaction within the proposed framework.

Corresponding author: Kang Song.

Zhengqing Yan, Yi Zhang, Fan Guo, and Kang Song are with the State Key Laboratory of Engines, Tianjin University, 300354 Tianjin, China. (e-mail: songkangtju@tju.edu.cn)

Xinyang Liu, ChengXun Jia, Junchen Wan, Yao Liu, Qi Liu, and Jihao Huang are with the Artificial Intelligence Center, Cylingo Group, 100080 Beijing, China.

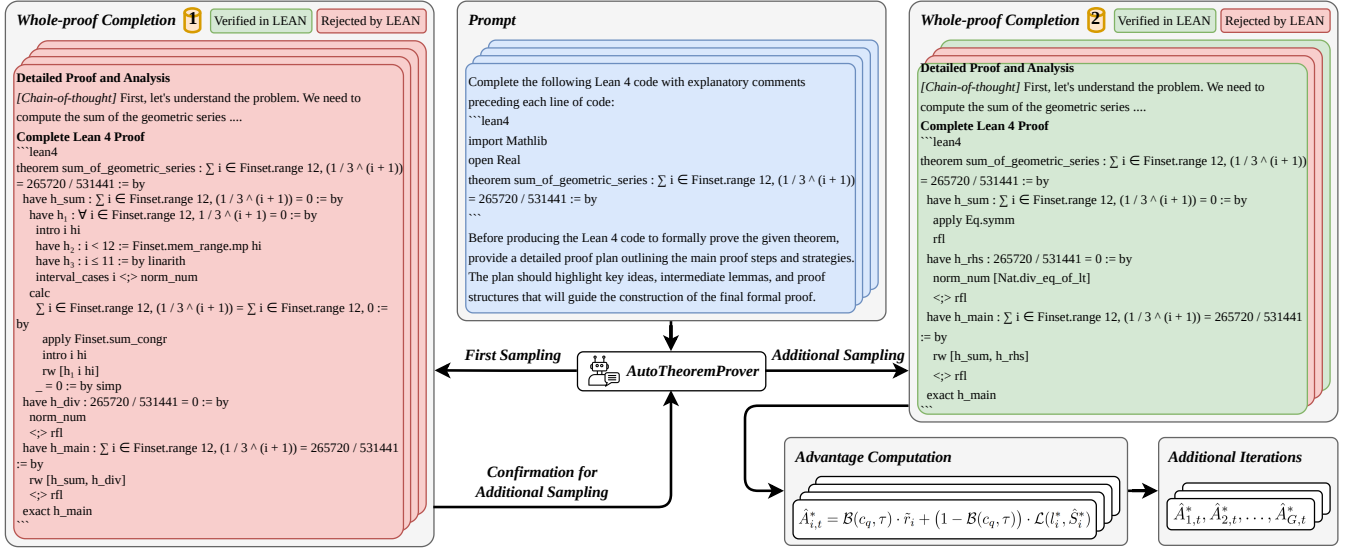


Fig. 1. The detailed training procedure of GDEPO: LLMs serve as auto-theorem provers by receiving a standardized prompt containing G identical problem instances, generating whole-proof completions, and verifying them through a Lean4 server [12]. A sample is deemed invalid if all outputs in the group are incorrect. For the same prompt, sampling continues up to a maximum number of attempts until at least one correct proof is obtained. When the within-group accuracy falls below a predefined threshold, the correctness feedback from the verifier contributes a sign term to the advantage function, while other signals determine its magnitude. For samples initially classified as invalid but later yielding valid proofs through subsequent sampling, an additional backward pass is performed to refine the model parameters.

II. RELATED WORK

A. Macroscopic Paradigm for Formal Theorem Proving

Existing algorithms aim to enhance proof success rates by innovating the inference paradigm.

The end-to-end generation paradigm trains models to directly output complete proof sequences that can be verified by formal verifiers such as Lean [1]–[3]. Representative works include DeepSeek-Prover [13], Goedel-Prover [14], and Kimina-Prover [15]. This paradigm leverages LLMs’ sequence generation capabilities, condensing the proof process into a single forward generation. It offers advantages of simple architecture and efficient reasoning. However, its performance is significantly constrained by the reliability of single-generation outputs, posing robustness challenges for complex theorems.

The proof search-based paradigm guides the model to incrementally construct proofs by exploring derivation paths at each step using feedback from a verifier. For instance, systems such as DeepSeek-Prover v1.5 [16], BFS-Prover [17], and ABEL [18] employ tree search algorithms—including Monte Carlo tree search or breadth-first search—to explore multiple proof trajectories and iteratively assemble valid proofs. This approach substantially enhances the robustness and provable scope of the system, albeit at the cost of considerable computational and time overhead.

To integrate the strengths of these paradigms or mitigate their inherent bottlenecks, a series of hybrid methods and auxiliary strategies have been proposed. These include leveraging retrieval-augmented generation (RAG) to introduce relevant theorems [19]; using informal proof sketches to guide formal step generation [19], [20]; and designing self-verification and iterative optimization loops [21]. The “verifier-in-the-loop” interactive strategy [22], [23] further highlights the value of iterative improvement through refined feedback. Additionally,

hybrid architectures like DSP+ [24] and Delta-Prover [25] adopt a two-stage method of “first generating a framework, then filling in details,” although their effectiveness typically relies on costly ultra-large-scale foundational models, such as DSP+ using the 671B parameter DeepSeek-R1 [26] or DeepSeek-V3 [27], while Delta-Prover utilizes Gemini [28].

Regardless of innovations in macro system architecture, ultimate performance remains limited by the underlying strategy’s ability to learn from formalized feedback. The efficiency, stability, and utilization of feedback signals by the algorithm directly determine whether the system can fully exploit data value and achieve reliable optimization.

B. Inadequate Adaptability of Policy Optimization Algorithms in Formal Theorem Proving

Inspired by informal LLMs in natural language processing, recent foundational work in formal theorem proving has adopted similar RL-based policy optimization strategies. Current formal theorem provers primarily rely on policy optimization algorithms originally developed for informal LLM training, such as Proximal Policy Optimization (PPO) [29], Direct Preference Optimization (DPO) [30], and Group Relative Policy Optimization (GRPO) [11], which is widely employed by state-of-the-art (SOTA) systems [5], [15], [22]. While these algorithms have demonstrated effectiveness in their native domains—such as language alignment and complex reasoning—they exhibit significant adaptation limitations when transferred to the formal theorem proving setting, where feedback is precise and binary.

1) *Limitations of the PPO and Reward Modeling Paradigm:* PPO and its associated reward-model-based paradigm rely on the assumption that the reward function can accurately and stably capture complex, composite qualities—such as

proof correctness and conciseness. In formal theorem proving, however, designing or learning such a reward model is highly challenging, often leading to training instability and reward overfitting, which in turn hinders effective multi-objective optimization.

2) *Limitations of the Direct Preference Optimization and Preference Optimization Paradigm:* DPO enhances training simplicity by directly leveraging preference data, thereby bypassing explicit reward model training. However, its optimization signal relies on global pairwise rankings, which are ill-suited to incorporate the highly structured, fine-grained feedback inherent to formal environments. Consequently, DPO struggles to support localized, incremental refinement of complex proof processes, limiting its effectiveness in interactive theorem proving scenarios that require stepwise correction.

3) *Limitations of the Group Relative Policy Optimization Paradigm:* GRPO has become the core optimization algorithm in current SOTA provers—such as DeepSeek-Prover-V2 [22], Kimina-Prover [15], and Goedel-Prover-V2 [5]—due to its elimination of a separate reward model and computational efficiency. However, its fundamental mechanism, which relies on relative comparisons among samples within a group, inherently conflicts with the absolute correctness criterion demanded by formal verification. This tension manifests in two critical issues. First, when composite rewards are employed, GRPO’s advantage computation may assign negative advantages to otherwise correct proof trajectories due to sub-optimal scores in other reward components—a mathematical possibility rigorously established in Section VI. To avoid this, practitioners often resort to binary rewards alone, thereby forfeiting the core capability of RL to align large language model outputs with nuanced human preferences, such as proof conciseness or elegance. Second, GRPO exhibits low data utilization efficiency: in batches containing a high proportion of challenging samples, using a single binary reward frequently results in zero advantages for all trajectories within a group. Consequently, all sampled attempts that fail to produce a valid proof are collectively discarded, wasting valuable training data. To mitigate these risks, existing SOTA systems [5], [15], [22] adopt a conservative strategy—using only binary rewards and deliberately forgoing the potential benefits of composite rewards. Moreover, data batches comprising exclusively correct or incorrect samples are often discarded outright [31]. These compromises yield dual adverse consequences: (i) the precise and rich feedback from formal verifiers remains underutilized, and (ii) the already scarce high-quality training data suffers from further reduced effective usage, impeding the model’s ability to learn from challenging examples. Additionally, the use of a fixed number of optimization iterations treats all samples uniformly, ignoring inherent differences in their learning value. As a result, the current training framework leaves considerable room for more efficient exploitation of formal proof data.

In summary, the inherent incompatibility between existing policy optimization algorithms—particularly GRPO, which serves as the de facto standard—and the formal verification environment constitutes a fundamental bottleneck that impedes efficient data utilization, reliable multi-objective optimization,

and effective learning from challenging examples. Developing a novel optimization framework that retains computational efficiency while fundamentally resolving these conflicts has thus become pivotal to advancing the field.

The overall architecture of the GDEPO framework and its comparison with conventional paradigms are illustrated in Fig. 2. The informal large language model RL paradigm, depicted in Fig. 2a, relies on a trained reward model to generate scalar rewards. However, such rewards lack the precise binary signal required to guarantee formal correctness. In contrast, the standard formal ATP paradigm, shown in Fig. 2b, employs a Lean verifier as the ground-truth judge but inherits two rigid design choices from generic RL: (i) a single-round sampling mechanism that struggles to explore low-probability correct solutions for complex problems, and (ii) a fixed number of iterations applied uniformly across all training samples, disregarding their varying learning utility. Moreover, the advantage estimation in this paradigm faces a dilemma: using a composite reward function often leads to misaligned gradient directions, whereas relying solely on the binary correctness reward results in poor data efficiency and weakens the ability of RL optimization to reflect desired output preferences.

As shown in Fig. 2c, the GDEPO algorithm builds upon the GRPO framework with several key enhancements. During training, the framework identifies ineffective samples and performs additional rollouts until valid ones are obtained, thereby maximizing data utilization. It then computes advantages using a redesigned function that enables proper integration of composite rewards for policy optimization. Finally, the number of policy update iterations is dynamically adjusted based on the difficulty of each sample, accelerating learning on challenging instances.

III. GROUP DUAL-DYNAMIC AND EQUAL-RIGHT ADVANTAGE POLICY OPTIMIZATION

GDEPO was proposed to address the aforementioned limitations of standard RL in formal theorem proving. The framework simultaneously improves data efficiency and optimization rationality.

As illustrated in Fig. 3, GDEPO overcomes these design constraints through two dynamic modules and a novel advantage computation method. The first module, *dynamic additional sampling*, actively increases the number of rollouts until a valid proof is found, thereby maximizing the utility of each training instance. The second module, *equal-right advantage*, decouples the verifier’s authoritative binary correctness signal from auxiliary quality-based rewards, ensuring that policy updates follow a theoretically sound optimization direction. The third component, *dynamic additional iterations*, allocates extra policy update steps based on the empirical difficulty of each sample. Together, these components form an integrated adaptive learning loop that concentrates exploration and computational resources on the most informative and challenging proof trajectories, leading to robust policy improvement and efficient data utilization.

The implementation details of these three core modules are elaborated below.

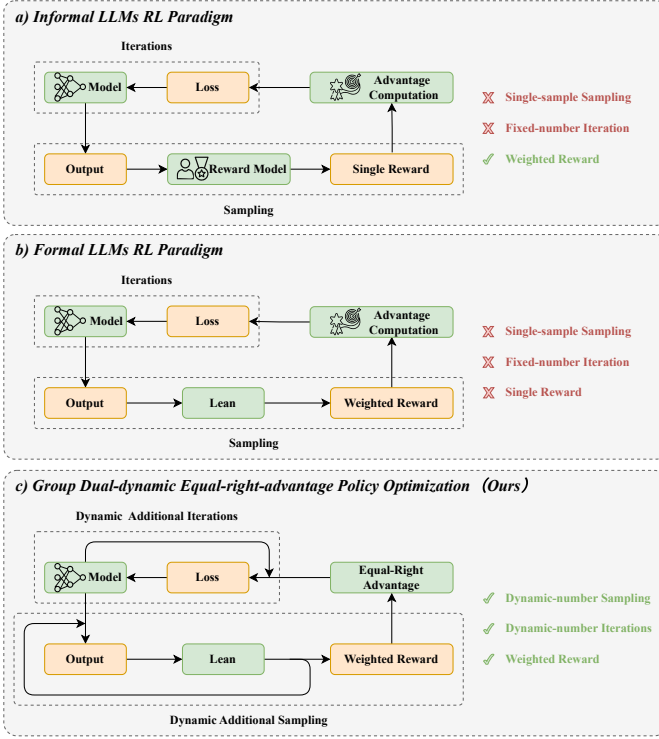


Fig. 2. Overall architecture of the GDEPO framework and its comparison with conventional paradigms.

A. Dynamic Additional Sampling

Standard GRPO performs only a single round of sampling per query. When handling challenging samples, the model may assign low probabilities to correct solutions [32]. Under this fixed single-round scheme, if all sampled outputs are incorrect, the resulting batch contains no positive learning signal. Discarding such batches not only wastes computational resources but also overlooks potentially valid candidates with low generation probabilities. To mitigate this issue, dynamic additional sampling is introduced to enhance the exploration of low-probability correct solutions.

The module follows a simple yet efficient design: if the initial sampling for a query yields no correct output, the system performs additional sampling on the same query until either a valid output is obtained or a preset maximum number of attempts is reached. The detailed pipeline is summarized in Algorithm1. For a given query q , the set of outputs from the k -th sampling round is denoted as follows:

$$\mathcal{G}_q^{(k)} = \{o_1^{(k)}, o_2^{(k)}, \dots, o_G^{(k)}\}, \quad (1)$$

where G denotes the fixed number of outputs per group. This output group corresponds to a core binary reward set

$$\mathcal{L}_q^{(k)} = \{l_1^{(k)}, l_2^{(k)}, \dots, l_G^{(k)}\}, \quad (2)$$

with each $l_i^{(k)} \in \{1, -1\}$, where 1 indicates a correct output and -1 an incorrect one (i.e., the Lean4 reward), and an auxiliary reward set

$$\mathcal{R}_q^{(k)} = \{\mathbf{r}_1^{(k)}, \mathbf{r}_2^{(k)}, \dots, \mathbf{r}_G^{(k)}\}, \quad (3)$$

where each $\mathbf{r}_i^{(k)} = (r_{i,1}^{(k)}, r_{i,2}^{(k)}, \dots, r_{i,K}^{(k)})$ is a K -dimensional auxiliary reward vector with components satisfying $r_{i,j}^{(k)} \in [0, 1]$ for all $j = 1, \dots, K$.

Correctness is our primary criterion; we aim to ensure that among the G trajectories generated for query q , at least one is correct to facilitate effective model optimization. Thus, the dynamic sampling terminates when either a correct output exists in the group, i.e., $\exists l_i^{(k)} = 1$, or the number of sampling iterations reaches the maximum limit n . The final valid output group for query q is denoted as \mathcal{G}_q^* , along with its associated valid rewards \mathcal{L}_q^* and \mathcal{R}_q^* . Formally, this is expressed as

$$\mathcal{G}_q^* = \mathcal{G}_q^{(k^*)}, \quad (4a)$$

$$\mathcal{L}_q^* = \mathcal{L}_q^{(k^*)}, \quad (4b)$$

$$\mathcal{R}_q^* = \mathcal{R}_q^{(k^*)}. \quad (4c)$$

where $k^* = \min\{k \mid k = n \text{ or } \exists l_i^{(k)} = 1, k \in [0, n], k \in \mathbb{Z}\}$; $q \sim P(Q)$ denotes a single problem sampled from the distribution of mathematical theorem-proving tasks; $l_i^{(k)} \in \{1, -1\}$ indicates the binary correctness label (with 1 denoting correct and -1 denoting incorrect) associated with the i -th trajectory in the k -th sampling; $n \in \mathbb{Z}$ is the user-specified maximum number of sampling (e.g., $n = 3$).

Algorithm 1 Dynamic Additional Sampling.

Input: maximum number of sampling $n \in \mathbb{Z}$, the query q
Output: the number of sampling k , valid trajectory group \mathcal{G}_q^* , core reward \mathcal{L}_q^* , auxiliary reward \mathcal{R}_q^*

- 1: initialize $k \leftarrow 0$
- 2: **for** $k = 0, 1, \dots, n$ **do**
- 3: do sampling by **Eq.1-3** to get $\mathcal{G}_q^{(k)}, \mathcal{L}_q^{(k)}, \mathcal{R}_q^{(k)}$
- 4: update the counter $k \leftarrow k + 1$
- 5: **if** $\exists l_i^{(k)} = 1$ **then**
- 6: break
- 7: **end**
- 8: **end**
- 9: do store the latest valid value by **Eq.4** to get $\mathcal{G}_q^*, \mathcal{L}_q^*, \mathcal{R}_q^*$
- 10: **return** $k, \mathcal{G}_q^*, \mathcal{L}_q^*, \mathcal{R}_q^*$

B. Equal-Right Advantage

The *equal-right advantage* is introduced to resolve a fundamental conflict that arises when applying GRPO to formal theorem proving tasks. Standard GRPO computes advantage values through intra-group comparisons. As shown in SectionVI, when composite rewards are used, it is mathematically possible for a trajectory verified as correct by Lean to receive a negative advantage due to unfavorable auxiliary rewards. This can cause the optimizer to suppress already-validated correct solutions, leading to training instability.

The detailed code pipeline is summarized in Algorithm2. Equal-right advantage decouples the supervision signal: the sign of the advantage—i.e., the direction of policy update—is determined solely by the binary label from the verifier, while auxiliary rewards modulate only the magnitude of the advantage—i.e., the update strength. This mechanism guarantees

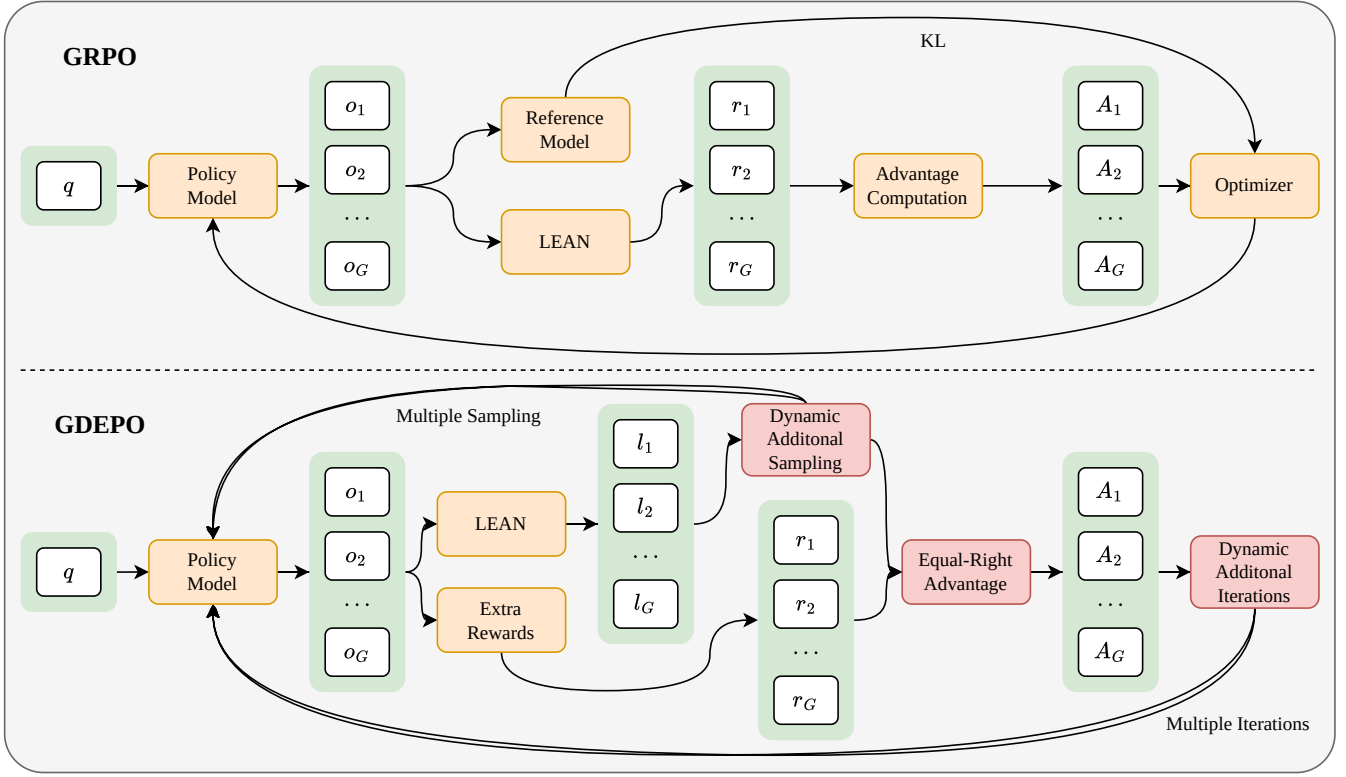


Fig. 3. Overall training framework of GDEPO in comparison with GRPO.

that all correct proofs receive positive signals and all incorrect ones receive negative signals, preserving the authority of verification outcomes while enabling multi-objective reward shaping. Importantly, it yields correct policy update directions even when all G trajectories for a query are either entirely correct or entirely incorrect.

Furthermore, the module adapts to sample difficulty: when the passing rate of sampled trajectories is low, equal-right advantage is activated to prioritize proof correctness; once the passing rate exceeds a preset threshold τ , the algorithm reverts to the standard GRPO advantage computation, allowing auxiliary rewards to refine proof quality within a reliably correct solution set. The equal-right advantage is computed as follows:

$$\hat{A}_{i,t}^* = \begin{cases} \tilde{r}_i, & c_q > \tau, \\ l_i^* \cdot \mathcal{L}(l_i^*, \hat{S}_i^*), & c_q \leq \tau, \end{cases} \quad (5a)$$

$$\mathcal{L}(l_i^*, \hat{S}_i^*) = \frac{l_i^* + 1}{2} \cdot \hat{S}_i^* + \frac{1 - l_i^*}{2} \cdot (1 - \hat{S}_i^*), \quad (5b)$$

$$\hat{S}_i^* = \begin{cases} 0.5 & \text{if } S_{\max}^* = S_{\min}^*, \\ \frac{S_i^* - S_{\min}^*}{S_{\max}^* - S_{\min}^*} & \text{otherwise.} \end{cases} \quad (5c)$$

Here, t denotes the token index, and $\hat{A}_{i,t}^*$ remains constant across all tokens within the same trajectory; $c_q \in [0, 1]$ denotes the pass rate of the query q ; $\tau \in (0, 1)$ is a predefined threshold on pass rate; $\tilde{r}_i = \frac{S_i^* - \text{mean}(S^*)}{\text{std}(S^*)}$ represents the normalized advantage of the i -th trajectory as used in conventional GRPO, where $S_i^* = \sum_{k=1}^K w_k \cdot r_{i,k}^*$ is the weighted sum of

auxiliary rewards for trajectory i , $\text{mean}(S^*)$ and $\text{std}(S^*)$ are the mean and standard deviation of $\{S_j^*\}_{j=1}^G$ over the valid output group, respectively; $l_i^* \in \{1, -1\}$ is the core binary correctness label for the i -th trajectory in the valid group (1 for correct, -1 for incorrect); $r_{i,k}^* \in [0, +\infty)$ is the k -th non-negative auxiliary reward associated with trajectory i ($k \geq 1$); $w = (w_1, w_2, \dots, w_K)$ is a weight vector for auxiliary rewards satisfying $w_k \geq 0$ and $\sum_{k=1}^K w_k = 1$; $S_{\max}^* = \max_{j=1, \dots, G} S_j^*$ and $S_{\min}^* = \min_{j=1, \dots, G} S_j^*$ denote the maximum and minimum of the auxiliary reward sums within the valid group; and \hat{S}_i^* is the min-max normalized value of S_i^* mapped into $[0, 1]$.

Finally, T_i denotes the token length of the i -th trajectory, with all tokens in the trajectory sharing the same advantage value $\hat{A}_{i,t}^*$. \mathcal{G}_q^* , \mathcal{L}_q^* , \mathcal{R}_q^*

C. Dynamic Additional Iterations

Although the dynamic additional sampling module enhances the exploration of low-probability correct solutions, it introduces a new issue of sample heterogeneity: proofs obtained directly in the initial sampling and those discovered only after repeated exploration possess markedly different instructional values for model optimization. The latter—requiring sustained search to succeed—deserve deeper RL attention. Applying identical single-step gradient updates to both cases fails to exploit the richer learning potential of the latter.

To address this, *dynamic additional iterations* are proposed to allocate computational resources proportionally to each sample's learning value. The detailed code pipeline is

Algorithm 2 Equal-Right Advantage.

Input: valid trajectory group $\mathcal{G}_q^{(*)}$, core binary reward \mathcal{L}_q^* , auxiliary reward \mathcal{R}_q^* , weights of auxiliary rewards $w = (w_1, \dots, w_K)$, the pass rate of the query c_q , accuracy threshold τ

Output: advantage value list of the query $\hat{\mathcal{A}}_{\text{list}}^*$

- 1: do weighted auxiliary rewards computation to get $S_{\text{all}}^* \leftarrow \{\sum_{k=1}^K w_k \cdot r_{i,k} \mid i = 1, \dots, G\}$
- 2: **for** $i = 1$ **to** G **do**
- 3: do advantage value per token computation by **Eq.5** to get $\hat{A}_{i,t}$
- 4: do advantage values for each token aggregate to get $\hat{\mathcal{A}}_{\text{list}}^*.append(\hat{A}_{i,t}^*)$
- 5: **end**
- 6: **return** $\hat{\mathcal{A}}_{\text{list}}^*$

summarized in Algorithm3. The principle is straightforward: easy queries (correct on the first attempt) and persistently unsolvable hard queries undergo only one update iteration, whereas medium-difficulty queries—those that yield a correct proof only after multiple sampling rounds—are subjected to m iterations to accelerate optimization. Formally, for a query q , if its valid output set \mathcal{G}_q^* contains at least one correct trajectory and was not produced in the first sampling round, then all G trajectories for q are used in m consecutive policy updates. The overall objective function is expressed as:

This design adaptively concentrates computational effort on parameter updates with higher pedagogical value—particularly those arising from successful multi-round searches. Consequently, the model more rapidly internalizes knowledge for solving theorems that are challenging yet solvable.

$$\mathcal{J}(\theta) = \mathbb{E}_{q \sim P(Q)} \left[\frac{1}{GT_i} \sum_{i=1}^{G, T_i} \min[\rho_{i,t}^{(s)} \hat{A}_{i,t}^*, \bar{\rho}_{i,t}^{(s)} \hat{A}_{i,t}^*] \right] \quad (6)$$

where the auxiliary operators are defined as

$$\rho_{i,t}^{(s)} = \frac{\pi_{\theta^{(s)}}(o_{i,t}^* \mid q, o_{i,<t}^*)}{\pi_{\theta_{\text{old}}^{(s)}}(o_{i,t}^* \mid q, o_{i,<t}^*)}, \quad (7a)$$

$$\bar{\rho}_{i,t}^{(s)} = \text{clip}(\rho_{i,t}^{(s)}, 1 - \varepsilon_{\text{low}}, 1 + \varepsilon_{\text{high}}). \quad (7b)$$

Here, $\rho_{i,t}^{(s)}$ denotes the policy ratio for the t -th token of the i -th trajectory during the s -th iteration; $\mathcal{C}(x) = \text{clip}(x, 1 - \varepsilon_{\text{low}}, 1 + \varepsilon_{\text{high}})$ is an asymmetric clipping function with user-defined bounds $\varepsilon_{\text{low}}, \varepsilon_{\text{high}} > 0$.

IV. DATASET AND TRAINING

A. Dataset for Training

The experiments are conducted on the publicly available Lean4 [2] formalized mathematical theorem dataset. To rigorously evaluate GDEPO’s core capability—learning from challenging samples—we construct a targeted high-difficulty training set. The data are sourced from FineLeanCorpus [33], a high-quality dataset comprising formally verified propositions with broad domain coverage and inherently high difficulty. To further isolate highly challenging instances, we use

Algorithm 3 Dynamic Additional Iterations.

Input: advantage value list of the query $\hat{\mathcal{A}}_{\text{list}}$, the number of sampling k , the number of iterations m , upper and lower bounds on the clipping ratio $\varepsilon_{\text{high}}$, lower bounds on the clipping ratio ε_{low} , core binary reward \mathcal{L}_q^*

Output: updated policy π_{θ}

- 1: **if** $\exists l_i^{(*)} = 1$ **and** $k > 1$ **then**
- 2: **for** iter = 0, 1, ..., m **do**
- 3: do policy updating with loss by **Eq.6-7** to get π_{θ}
- 4: **else**
- 5: do policy updating with loss by **Eq.6-7** to get π_{θ}
- 6: **return** π_{θ}

the pass@32 performance of the DeepSeek-Prover-V2-671B model as a filtering criterion, retaining only those samples for which no correct proof is found across 32 independent sampling attempts.

B. Benchmarks

We employ three widely adopted benchmarks for evaluating the mathematical theorem-proving performance of LLMs, ordered by increasing difficulty.

1) *MiniF2F-test*: MiniF2F-test, the test split of MiniF2F [4], consists of 244 Lean-formalized problems derived from high school mathematical olympiads, including the American Mathematics Competitions (AMC), the American Invitational Mathematics Examination (AIME), and the International Mathematical Olympiad (IMO). In this study, we adopt the cleaned version of MiniF2F provided by the Kimina team [15], which ensures reliability through 13-gram decontamination, removal of duplicates, and correction of unsolvable instances.

2) *MathOlympiadBench*: MathOlympiadBench [5] raises the difficulty further by comprising 360 manually verified formal problems, each associated with a unique, complete, and Mathlib-compatible theorem along with an informal statement. The problems are drawn from the Compfiles database and the IMOSLLean4 codebase, forming a rigorously curated set of medium-to-high-difficulty proof tasks.

3) *PutnamBench*: PutnamBench [6] represents the most challenging evaluation in our study, featuring 644 university-level problems from the William Lowell Putnam Mathematical Competition held between 1962 and 2023. Covering algebra, analysis, number theory, geometry, combinatorics, probability, and set theory, this benchmark demands advanced mathematical insight and precise formal reasoning.

The aforementioned benchmarks collectively form a rigorous multi-level evaluation framework for assessing the model’s generalization capability across continuously varying levels of mathematical complexity.

C. Baselines

We compare GDEPO-Prover with three SOTA models representing leading paradigms in the field of ATP, ensuring a diverse evaluation across model architectures and optimization strategies.

1) *DeepSeek-Prover-V2*: DeepSeek-Prover-V2 [22] adopts a recursive subgoal decomposition paradigm. Its training process integrates multiple stages: problem decomposition and formalization using DeepSeek-V3; recursive subgoal solving with a 7 billion parameter model; curriculum learning for task generation; RL via GRPO algorithm, complemented by supervised fine-tuning and knowledge distillation.

2) *Kimina-Prover*: Kimina-Prover [15] emphasizes training stability through KL-constrained RL. It initializes via few-shot fine-tuning, featuring innovations such as automated formalization methods for dataset construction, specialized tokenized reasoning formats for aligning informal and formal reasoning, and techniques like format filtering and negative gradient dropping to enhance stability.

3) *Goedel-Prover-V2*: Goedel-Prover-V2 [5] is centered around scaffolded data synthesis and iterative self-correction. Key components include scaffolded data synthesis generating progressively challenging tasks, verifier-guided self-correction leveraging Lean compiler feedback for iterative proof correction, model averaging to mitigate output diversity decline in later training stages by blending model checkpoints, and hybrid GRPO RL incorporating dynamic sampling [31], combined with supervised fine-tuning for efficient theorem proving with smaller parameter sizes.

These benchmark models cover three core technical directions in ATP—modular decomposition, constraint optimization, and feedback-loop enabled synthetic data. By comparing GDEPO, which focuses on innovative training algorithms, against these models, we can precisely isolate the performance gains attributed to our proposed dynamic sampling and advantage estimation mechanisms.

D. Training Details

To ensure a fair comparison, all shared hyperparameters of the trainable models are standardized and uniformly configured. The GDEPO algorithm adopts Godel-Prover-V2-8B [5] as the base model and is enhanced within the Open-R1 algorithmic framework [34].

The learning rate is set to 1×10^{-6} , with a training batch size of 32 and an evaluation batch size of 128. Training is distributed using DeepSpeed ZeRO-3, with `bfloat16` precision and FlashAttention-2 enabled. Asymmetric clipping is applied to amplify updates from low-probability correct solutions, with $\epsilon_{\text{low}} = 0.2$ and $\epsilon_{\text{high}} = 0.28$ [31]. The optimizer is AdamW, and the learning rate follows a cosine schedule with a minimum learning rate, using a warmup ratio of 0.1. KL divergence constraints are removed during training to enhance exploration capability [5].

The number of training epochs is set to 2. The sign of the advantage function is determined solely by the correctness of the proof as judged by the Lean4 server [12]. The reward function assigns a +1 reward for a correct theorem-proving trajectory and a -1 penalty for an incorrect one [35], with this component weighted by 1. Additionally, two auxiliary penalties are applied: a repetition penalty in the range $(-1, 1)$ based on N-gram overlap (with $N = 5$), which yields positive rewards when no repetition occurs and negative rewards for

severe redundancy; and a smooth length penalty also in $(-1, 1)$, computed via a cosine function of the generated sequence length—short outputs receive rewards close to +1, while long outputs receive rewards approaching -1, ensuring a smooth transition across lengths. All three reward components share equal weights to encourage concise yet correct proofs while eliminating potential bias from unequal weighting. For all baseline methods, the sampling procedure, weighted reward computation, and advantage estimation follow standard practices without modification. In contrast, our proposed GDEPO family of models performs additional sampling only when encountering invalid training data and applies extra optimization to promote effective exploration. Outside such exploratory scenarios, GDEPO models operate identically to the baselines, adopting the same sampling strategy and reward weighting scheme.

All baselines use standard procedures for sampling, weighted reward computation, and advantage estimation. In contrast, GDEPO performs additional sampling and targeted optimization only when encountering invalid training data; otherwise, it follows the exact same pipeline as the baselines in non-exploration mode.

All reported results are averaged over 10 independent runs with distinct random seeds to ensure statistical reliability.

V. EXPERIMENTS

To comprehensively evaluate the effectiveness of our algorithm from multiple perspectives, our experiments comprised four components: (a) assessing the overall performance of our method; (b) evaluating its capability to leverage challenging training data; (c) examining the efficacy of the equal-right advantage module in utilizing composite rewards; and (d) analyzing the individual contribution of each module within the GDEPO framework.

A. Overall Performance Evaluation

To evaluate the overall performance of GDEPO, we trained GOEDEL-Prover-V2 on a dataset of 30,000 samples containing 30% challenging instances and selected the best-performing model as the representative of our method. Table I reports the performance of this model alongside SOTA baselines, including DeepSeek-Prover-V2 [22], Kimina-Prover [15], and Goedel-Prover-V2 [5], along with their variants of different parameter scales. To ensure that the performance improvement of GDEPO is not affected by uncertainties, the performance data of untrained SOTA models are obtained from their respective official teams. The results show that GDEPO consistently improves performance across all three benchmarks, with a notable 84% gain on the most challenging PutnamBench. This demonstrates that GDEPO can effectively unlock additional performance potential even in models that have approached their performance ceilings, highlighting its strong capability in learning from challenging samples.

B. Utilization Effect of Challenging Training Data Evaluation

To evaluate how effectively our method leverages challenging samples in the training data, we fixed the total number

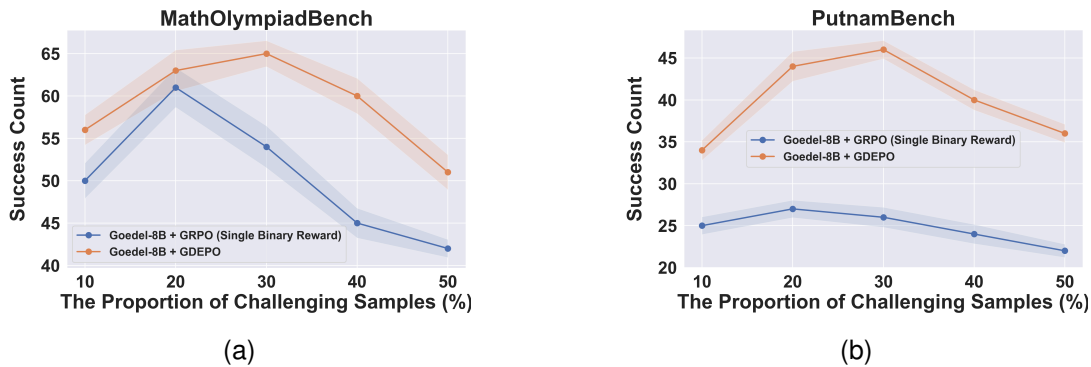


Fig. 4. Performance comparison of the same base model trained with GRPO using a single binary reward versus GDEPO employing composite rewards, under varying proportions of challenging samples: (a) performances on MathOlympiadBench; (b) performances on PutnamBench.

TABLE I
PERFORMANCE COMPARISON OF GDEPO-PROVER WITH EXISTING
SOTA MODELS AND THEIR VARIANTS ACROSS MODEL SIZES.

Model	MiniF2F-test	MathOlympiadBench	PutnamBench
	Pass Rate (%)	Number of Problem Solved	
DeepSeek-Prover-V2-7B	75.6	7	9
DeepSeek-Prover-V2-671B	82.4	50	22
Kimina-Prover-8B	78.3	26	15
Kimina-Prover-72B	84.0	58	24
Goedel-Prover-V2-8B	84.6	60	25
GDEPO-Prover-8B(Ours)	86.2	65	46

of training problems at 30,000 and constructed five datasets with varying proportions of challenging samples: 10%, 20%, 30%, 40%, and 50%. Fig.4a-4b compare the performance of the same base model trained using the standard GRPO method with a single binary reward against that trained with GDEPO employing a composite reward, across these different ratios of challenging data. The results show that GDEPO consistently outperforms GRPO, with the performance gap widening as the proportion of challenging samples increases. This indicates that GDEPO makes more effective use of difficult samples that the model initially fails to solve within a batch. Moreover, by performing additional sampling on such challenging instances that do not yield correct outputs on the first attempt, GDEPO effectively increases the equivalent batch size, thereby enhancing the probability of generating low-likelihood correct solutions and rapidly amplifying their output probabilities through the equal-right advantage.

C. Effectiveness of Equal-Right Advantage Evaluation

To assess the contribution of the equal-right advantage module to the effective utilization of composite rewards, we compare three variants: GRPO with a single binary reward, GRPO with composite rewards, and our proposed GDEPO. To ensure the best performance of the algorithms, GDEPO is trained on 30,000 training samples containing 30% challenging samples, while GRPO with two different reward configurations is trained on 30,000 samples containing 20% challenging samples. The composite reward function used in GRPO matches GDEPO exactly in both reward types and weights to eliminate any confounding effects from reward weighting. As shown in

TableII, GDEPO reduces both the average output length and repetition rate without compromising success rate, by properly computing the advantage based on composite rewards. In the table, “number of tokens” denotes the average token count across all completions, and “similarity rate” refers to the average 5-gram repetition rate. While directly applying composite rewards in GRPO also suppresses output length and redundancy, it incurs a noticeable drop in correctness—a critical metric. In contrast, GDEPO preserves correctness by using it to determine the sign of the advantage function, thereby ensuring a proper policy optimization direction, while leveraging auxiliary rewards to modulate the magnitude of policy updates and balance multiple objectives.

D. Ablation Evaluation

To evaluate the individual contributions of dynamic additional sampling, dynamic additional iterations, and the equal-right advantage module in GDEPO, we conduct an ablation study. All experiments are trained on a fixed dataset of 30,000 problems containing 30% challenging samples. TableIII presents the ablation results across three evaluation benchmarks. Since dynamic additional iterations depend on the outcomes of dynamic additional sampling, we do not test the iteration module in isolation. The results show that each component contributes to performance gains to varying degrees. Collectively, the ablation study confirms the importance of every module in the GDEPO framework.

VI. THE IMPORTANCE OF ADVANTAGE

This section provides a supplementary analysis of the GRPO algorithm [11], showing that the sign of the advantage solely determines the direction of change in the trajectory’s output probability. Furthermore, when a correctness-based reward is combined with other components in a composite reward function, it is mathematically possible for a correct trajectory to receive a negative advantage due to penalties from the auxiliary rewards.

TABLE II
PERFORMANCE COMPARISON OF THE EQUAL-RIGHT ADVANTAGE MODULE AGAINST GRPO WITH SINGLE BINARY REWARD AND GRPO WITH COMPOSITE REWARD FUNCTIONS.

Algorithm	MiniF2F-test			MathOlympiad Bench			Putnam Bench		
	Pass Rate (%) ↑	Tokens ↓	Simi. Rate (%) ↓	Prob. Solved ↑	Tokens ↓	Simi. Rate (%) ↓	Prob. Solved ↑	Tokens ↓	Simi. Rate (%) ↓
Goedel-Prover-V2-8B with GRPO (Single Binary Reward)	84.8	9640.89	49.29	61	28692.96	81.84	27	30148.48	85.23
Goedel-Prover-V2-8B with GRPO	83.2	7903.04	46.99	59	14906.10	75.59	24	26215.64	80.76
δ Perf.	-1.6	-1737.85	-2.30	-2	-13786.86	-6.25	-3	-3932.84	-4.47
Goedel-Prover-V2-8B with Equal-Right Advantage	85.3	9008.35	48.22	62	15632.41	77.33	31	28510.36	83.87
δ Perf.	+0.5	-632.54	-1.07	+1	-13060.55	-4.51	+4	-1638.12	-1.36

The performance difference relative to Goedel-Prover-V2-8B with GRPO (Single Binary Reward) is indicated as "δ Perf.". Tokens = Number of Tokens, Simi. Rate = Similarity Rate, Prob. Solved = Number of Problem Solved. Higher values are preferred for metrics marked with ↑, and lower values are preferred for those marked with ↓.

TABLE III

ABLATION STUDY RESULTS, SHOWING THE IMPACT OF EACH COMPONENT ON OVERALL PERFORMANCE.

Module			MiniF2F-test	MathOlympiadBench	PutnamBench
D.A.S.	E.R.A.	D.A.I.	Pass Rate (%)	Number of Problems Solved	
-	-	-	84.6	60	25
✓	-	-	84.9 (+0.3)	63 (+3)	36 (+11)
-	✓	-	85.3 (+0.7)	62 (+2)	31 (+6)
✓	-	✓	85.8 (+1.2)	64 (+4)	41 (+16)
✓	✓	✓	86.2 (+1.6)	65 (+5)	46 (+21)

The baseline is Godel-Prover-V2-8B. The dynamic additional sampling is indicated as "D.A.S.". The equal-right advantage is indicated as "E.R.A.". The dynamic additional iterations is indicated as "D.A.I.".

A. Advantage Sign as Determinant of Trajectory Probability Direction

The gradient of the objective function after removing the KL divergence is given by

$$\nabla \mathcal{J}(\theta) = \mathbb{E} \left[\frac{1}{GT_i} \sum_{i=1}^{G, T_i} \min[\nabla \rho_{i,t}^{(s)} \hat{A}_{i,t}^*, \nabla \bar{\rho}_{i,t}^{(s)} \hat{A}_{i,t}^*] \right] \quad (8)$$

where the auxiliary quantities are defined as

$$\rho_{i,t}^{(s)} = \frac{\pi_{\theta^{(s)}}(o_{i,t}^* | q, o_{i,<t}^*)}{\pi_{\theta_{\text{old}}^{(s)}}(o_{i,t}^* | q, o_{i,<t}^*)}, \quad (9a)$$

$$\bar{\rho}_{i,t}^{(s)} = \text{clip}(\rho_{i,t}^{(s)}, 1 - \varepsilon_{\text{low}}, 1 + \varepsilon_{\text{high}}). \quad (9b)$$

Here, $\pi_{\theta_{\text{old}}^{(s)}}(o_{i,t}^* | q, o_{i,<t}^*)$ denotes the probability under the old policy and remains constant with respect to θ . The expectation operator \mathbb{E} is representing expectation over the question distribution and the effective response groups sampled from the old policy $\mathbb{E}_{q \sim P(Q)}$. Consequently, it can be treated as a fixed quantity during differentiation. The gradients $\nabla \rho_{i,t}^{(s)}$ and $\nabla \bar{\rho}_{i,t}^{(s)}$ can be further decomposed:

$$\nabla \rho_{i,t}^{(s)} = \frac{\nabla \pi_{\theta^{(s)}}(o_{i,t}^* | q, o_{i,<t}^*)}{\pi_{\theta_{\text{old}}^{(s)}}(o_{i,t}^* | q, o_{i,<t}^*)}, \quad (10a)$$

$$\nabla \bar{\rho}_{i,t}^{(s)} = \text{clip}(\nabla \rho_{i,t}^{(s)}, 1 - \varepsilon_{\text{low}}, 1 + \varepsilon_{\text{high}}). \quad (10b)$$

At the first iteration, $\rho_{i,t}^{(s)} = 1$ and $\nabla \bar{\rho}_{i,t}^{(s)} = \nabla \rho_{i,t}^{(s)}$, rendering the clipping operation inconsequential. The gradient $\nabla \rho_{i,t}^{(s)}$ fundamentally reflects the alignment between the direction of change in the policy probability and the direction of parameter

update θ . Employing gradient ascent to maximize the objective function, the relationship between the sign of the advantage and the direction of change in the trajectory probability during the first iteration is illustrated in Fig.5. Moreover, it follows that when $\rho_{i,t}^{(s)} \neq 1$, its relative magnitude with respect to unity is uniquely determined by the sign of the advantage. Specifically, whenever $\rho_{i,t}^{(s)}$ exceeds the upper clipping bound, $\hat{A}_{i,t}^* > 0$ holds invariably, ensuring that the minimum operator always selects $\bar{\rho}_{i,t}^{(s)}$; the converse also holds symmetrically. Consequently, the objective function—after removal of the KL divergence term—and its gradient can be simplified.

$$\mathcal{J}(\theta) = \mathbb{E}_{q \sim P(Q)} \mathbb{E}_{\mathcal{G}_{q^*} \sim \pi_{\theta_{\text{old}}^{(s)}}} \left[\frac{1}{GT_i} \sum_{i=1}^{G, T_i} \hat{\rho}_{i,t}^{(s)} \hat{A}_{i,t}^* \right], \quad (11a)$$

$$\nabla \mathcal{J}(\theta) = \mathbb{E}_{q \sim P(Q)} \mathbb{E}_{\mathcal{G}_{q^*} \sim \pi_{\theta_{\text{old}}^{(s)}}} \left[\frac{1}{GT_i} \sum_{i=1}^{G, T_i} \nabla \hat{\rho}_{i,t}^{(s)} \hat{A}_{i,t}^* \right] \quad (11b)$$

where the auxiliary quantities are defined as

$$\hat{\rho}_{i,t}^{(s)} = \begin{cases} \rho_{i,t}^{(s)}, & \rho_{i,t}^{(s)} \in (1 - \varepsilon_{\text{low}}, 1 + \varepsilon_{\text{high}}) \\ \bar{\rho}_{i,t}^{(s)}, & \rho_{i,t}^{(s)} \notin (1 - \varepsilon_{\text{low}}, 1 + \varepsilon_{\text{high}}) \end{cases}, \quad (12a)$$

$$\nabla \hat{\rho}_{i,t}^{(s)} = \begin{cases} \nabla \rho_{i,t}^{(s)}, & \rho_{i,t}^{(s)} \in (1 - \varepsilon_{\text{low}}, 1 + \varepsilon_{\text{high}}) \\ 0, & \rho_{i,t}^{(s)} \notin (1 - \varepsilon_{\text{low}}, 1 + \varepsilon_{\text{high}}) \end{cases}. \quad (12b)$$

It is proven that the min function, in extreme cases, enforces the gradient to zero, thereby preventing excessive deviation in the output probability of the trajectory across multiple iterations. In subsequent iterations, even when $\rho_{i,t}^{(s)} \neq 1$, the sign of the advantage and the direction of change in the trajectory's output probability remain consistent with the procedure illustrated in Fig.5.

In summary, the sign of the advantage function uniquely determines the direction of change in the trajectory output probability.

B. Possibility of Negative Advantages on Correct Trajectories under Composite Rewards

The advantage function in the GRPO algorithm is computed as follows:

$$\hat{A}_{i,t} = \tilde{r}_i = \frac{r_i - \text{mean}(r)}{\text{std}(r)} \quad (13)$$

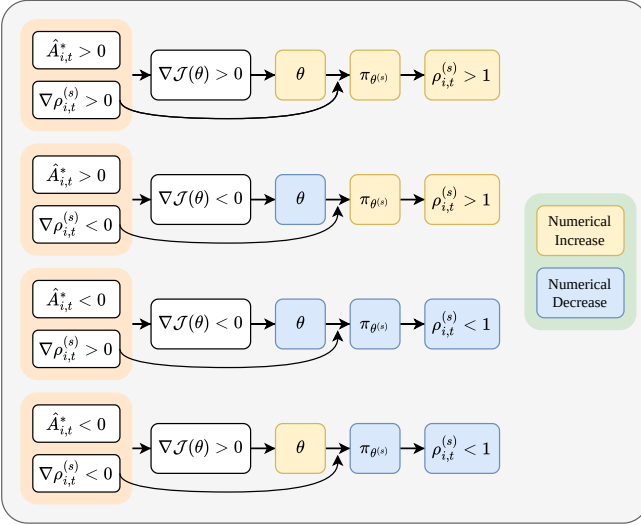


Fig. 5. Relationship between the sign of advantage and the direction of change in trajectory output probabilities.

where r_i denotes the total reward of the i -th output. $\text{mean}(r)$ and $\text{std}(r)$ represent the mean and standard deviation of the rewards within the group, respectively. The advantage function for all tokens corresponding to a given output is identical and equal to the normalized total reward of that output (i.e., $\hat{A}_{i,t}$ remains constant across all timesteps t for the same output).

For a query q , a sampled trajectory is denoted as $\mathcal{G}_q = \{o_1, o_2, \dots, o_G\}$. The correctness binary reward is represented by $\mathcal{L}_q = \{l_1, l_2, \dots, l_G\}$, where each $l_i \in \{0, 1\}$, with 1 indicating a correct output and 0 an incorrect one. The auxiliary reward is denoted as $\mathcal{R}_q = \{\mathbf{r}_1, \mathbf{r}_2, \dots, \mathbf{r}_G\}$, where each $\mathbf{r}_i = (r_{i,1}, r_{i,2}, \dots, r_{i,K})$ is a K -dimensional auxiliary reward vector whose components satisfy $r_{i,j} \in [0, 1]$ for all $j = 1, \dots, K$.

The weight assigned to the correctness binary reward is $\alpha > 0$, and the weights for the auxiliary rewards are given by $w = (w_1, \dots, w_K)$, subject to the constraint $\sum_{j=1}^K w_j = 1$. The raw weighted reward for output $o_i^{(k)}$ is defined as $s_i^{(k)} = \alpha \cdot l_i^{(k)} + \sum_{j=1}^K w_j \cdot r_{i,j}^{(k)}$, with its empirical mean and standard deviation given respectively by $\mu_s^{(k)} = \frac{1}{G} \sum_{i=1}^G s_i^{(k)}$ and $\sigma_s^{(k)} = \sqrt{\frac{1}{G-1} \sum_{i=1}^G (s_i^{(k)} - \mu_s^{(k)})^2}$. Eq.13 can thus be reformulated as follows:

$$\hat{A}_i = \frac{s_i - \mu_s}{\sigma_s} \quad (14)$$

The sign of the advantage is determined by the numerator: $\hat{A}_i < 0 \iff s_i < \mu_s$.

To simplify the analysis while maintaining generality, the following reasonable assumptions are introduced. 1) *Reward Independence Assumption*: The correctness indicator l_i and the auxiliary reward vector \mathbf{r}_i are mutually independent, i.e., $\mathbb{E}[l_i r_{i,j}] = \mathbb{E}[l_i] \mathbb{E}[r_{i,j}]$ for all j . 2) *Non-degeneracy Within Group Assumption*: The expected correctness rate satisfies $p = \mathbb{E}[l_i] \in (0, 1)$, and the expected auxiliary rewards satisfy $\mu_j = \mathbb{E}[r_{i,j}] \in (0, 1)$ for all j , ensuring that both

correct and incorrect outputs exist within the group. Moreover, the standard deviation of the total reward within the group satisfies $\sigma_s > 0$, thereby excluding the degenerate case where all outputs receive identical rewards.3) *Non-zero Weight Assumption*: The weight assigned to the correctness reward satisfies $\alpha > 0$, and each auxiliary reward weight satisfies $w_j > 0$, guaranteeing that both reward components contribute non-trivially to the total reward.

The outputs within the group are partitioned into two subsets based on correctness: the set of correct outputs $\mathcal{G}_1 = \{o_i \mid l_i = 1\}$, with cardinality $G_1 = pG$ and weighted average auxiliary reward $\bar{r}_1 = \sum_{j=1}^K w_j \cdot \frac{1}{G_1} \sum_{o_i \in \mathcal{G}_1} r_{i,j}$; and the set of incorrect outputs $\mathcal{G}_0 = \{o_i \mid l_i = 0\}$, with cardinality $G_0 = (1-p)G$ and weighted average auxiliary reward $\bar{r}_0 = \sum_{j=1}^K w_j \cdot \frac{1}{G_0} \sum_{o_i \in \mathcal{G}_0} r_{i,j}$.

Consequently, the group-level mean of the total reward can be decomposed as follows:

$$\mu_s = \alpha p + p\bar{r}_1 + (1-p)\bar{r}_0 \quad (15)$$

The average total reward of the correct subset is given by:

$$\mu_{s,1} = \alpha + \bar{r}_1 \quad (16)$$

There exists a correct output $o_i \in \mathcal{G}_1$ such that $\hat{A}_i < 0$ if and only if:

$$\mu_{s,1} < \mu_s \quad (17)$$

The necessity is proved as follows. Suppose there exists $o_i \in \mathcal{G}_1$ for which $\hat{A}_i < 0$. Then, by definition of the advantage function, $s_i < \mu_s$. Since $\mu_{s,1} = \frac{1}{G_1} \sum_{o_i \in \mathcal{G}_1} s_i$ denotes the average total reward over all correct outputs, if $s_i \geq \mu_s$ held for every $o_i \in \mathcal{G}_1$, it would follow that $\mu_{s,1} \geq \mu_s$, leading to a contradiction. Hence, it must be that $\mu_{s,1} < \mu_s$.

For sufficiency, suppose $\mu_{s,1} < \mu_s$. By the definition of the arithmetic mean, there necessarily exists at least one $o_i \in \mathcal{G}_1$ such that $s_i < \mu_s$. Given that $\sigma_s > 0$ —which follows from the non-degeneracy of rewards within the group (as identical rewards would render the advantage function undefined)—it follows that $\hat{A}_i < 0$. Consequently, there exists a correct output exhibiting a negative advantage.

In summary, when a correctness-based reward is incorporated into a composite reward structure, it is mathematically possible for a correct trajectory to yield a negative advantage due to the influence of other reward components.

VII. CONCLUSION

This paper addresses critical limitations in current RL based ATP methods concerning training efficiency and optimization direction by proposing the GDEPO framework. GDEPO systematically enhances the learning efficacy of LLMs in formal reasoning through three key mechanisms. First, it leverages the Lean verifier to precisely identify and discard entirely invalid training samples while actively exploring potentially correct proof paths via a supplementary sampling strategy. Second, it introduces the equal-right advantage mechanism, which preserves the binary correctness signal from the verifier as the primary optimization direction while integrating multidimensional auxiliary rewards to enrich the policy gradient

representation. Third, it applies dynamic-iteration backpropagation on challenging samples that initially fail but eventually succeed, accelerating the model’s mastery of difficult yet solvable problems.

We conduct comprehensive experiments on three progressively challenging formal mathematical benchmarks: MinF2F-test, MathOlympiadBench, and PutnamBench. Results demonstrate that GDEPO significantly outperforms existing GRPO-based training paradigms, achieving substantial gains in both proof success rate and data utilization efficiency. Ablation studies further confirm that all three components are essential and act synergistically.

This work not only delivers a more efficient and robust training framework for LLM-driven ATP systems but also offers a novel perspective on designing RL algorithms for tasks equipped with precise verification mechanisms. With the advancement of AI, nearly all collectible training data have already been exhausted, and the difficulty of acquiring or generating high-value training data continues to rise. While prior research has largely focused on increasing data quantity and quality and on crafting sophisticated reward functions, we argue that future efforts should place equal emphasis on maximizing the utility of existing data and on developing domain-informed strategies for computing trajectory advantages in RL applications.

REFERENCES

- [1] L. de Moura, S. Kong, J. Avigad, F. Van Doorn, and J. von Raumer, “The Lean Theorem Prover (System Description),” in *Proc. Int. Conf. Automated Deduction (CADE)*. Springer, 2015, pp. 378–388.
- [2] L. de Moura and S. Ullrich, “The Lean 4 Theorem Prover and Programming Language,” in *Proc. Int. Conf. Automated Deduction (CADE)*. Springer, 2021, pp. 625–635.
- [3] H. Ying, Z. Wu, Y. Geng, J. Wang, D. Lin, and K. Chen, “Lean Workbook: A large-scale Lean problem set formalized from natural language math problems,” in *Proc. 38th Conf. Neural Information Processing Systems (NeurIPS) Datasets and Benchmarks Track*, 2024. [Online]. Available: <https://openreview.net/forum?id=Vcw3vzjHDb>
- [4] K. Zheng, J. M. Han, and S. Polu, “miniF2F: a cross-system benchmark for formal olympiad-level mathematics,” in *Proc. Int. Conf. Learning Representations (ICLR)*, 2022. [Online]. Available: <https://openreview.net/forum?id=9ZPegFuFTFv>
- [5] Y. Lin, S. Tang, B. Lyu, Z. Yang, J.-H. Chung, H. Zhao, L. Jiang, Y. Geng, J. Ge, J. Sun *et al.*, “Goedel-Prover-V2: Scaling Formal Theorem Proving with Scaffolded Data Synthesis and Self-Correction,” *arXiv preprint arXiv:2508.03613*, 2025.
- [6] G. Tsoukalas, J. Lee, J. Jennings, J. Xin, M. Ding, M. Jennings, A. Thakur, and S. Chaudhuri, “PutnamBench: Evaluating Neural Theorem-Provers on the Putnam Mathematical Competition,” in *Proc. 38th Conf. Neural Information Processing Systems (NeurIPS) Datasets and Benchmarks Track*, vol. 37, 2024, pp. 11 545–11 569.
- [7] G. Gao, Y. Wang, J. Jiang, Q. Gao, Z. Qin, T. Xu, and B. Dong, “Herald: A Natural Language Annotated Lean 4 Dataset,” in *Proc. 13th Int. Conf. Learning Representations (ICLR)*, 2025. [Online]. Available: <https://openreview.net/forum?id=Se6MgCtRhZ>
- [8] J. Hu, T. Zhu, and S. Welleck, “miniCTX: Neural Theorem Proving with (Long-)Contexts,” in *Proc. 13th Int. Conf. Learning Representations (ICLR)*, 2025. [Online]. Available: <https://openreview.net/forum?id=KIgaAqEFHW>
- [9] H. Wang, H. Xin, Z. Liu, W. Li, Y. Huang, J. Lu, Z. YANG, J. Tang, J. Yin, Z. Li, and X. Liang, “Proving Theorems Recursively,” in *Proc. 38th Annual Conf. Neural Information Processing Systems (NeurIPS)*, 2024. [Online]. Available: <https://openreview.net/forum?id=yAa5192TtQ>
- [10] T. H. Trinh, Y. Wu, Q. V. Le, H. He, and T. Luong, “Solving olympiad geometry without human demonstrations,” *Nature*, vol. 625, no. 7995, pp. 476–482, 2024.
- [11] Z. Shao, P. Wang, Q. Zhu, R. Xu, J. Song, X. Bi, H. Zhang, M. Zhang, Y. Li, Y. Wu, and D. Guo, “DeepSeekMath: Pushing the Limits of Mathematical Reasoning in Open Language Models,” *arXiv preprint arXiv:2402.03300*, 2024.
- [12] M. D. Santos, H. de Saxcé, H. Wang, M. Baksys, M. Unsal, J. Liu, Z. Liu, and J. LI, “Kimina Lean Server: A High-Performance Lean Server for Large-Scale Verification,” in *Proc. 5th Workshop on Mathematical Reasoning and AI at NeurIPS 2025*, 2025. [Online]. Available: <https://openreview.net/forum?id=orPt2nxLoC>
- [13] H. Xin, D. Guo, Z. Shao, Z. Ren, Q. Zhu, B. Liu, C. Ruan, W. Li, and X. Liang, “DeepSeek-Prover: Advancing Theorem Proving in LLMs through Large-Scale Synthetic Data,” *arXiv preprint arXiv:2405.14333*, 2024.
- [14] Y. Lin, S. Tang, B. Lyu, J. Wu, H. Lin, K. Yang, J. Li, M. Xia, D. Chen, S. Arora, and C. Jin, “Goedel-Prover: A Frontier Model for Open-Source Automated Theorem Proving,” *arXiv preprint arXiv:2502.07640*, 2025.
- [15] H. Wang, M. Unsal, X. Lin, M. Baksys, J. Liu, M. D. Santos, F. Sung, M. Vinyes, Z. Ying, Z. Zhu *et al.*, “Kimina-Prover Preview: Towards Large Formal Reasoning Models with Reinforcement Learning,” *arXiv preprint arXiv:2504.11354*, 2025.
- [16] H. Xin, Z. Ren, J. Song, Z. Shao, W. Zhao, H. Wang, B. Liu, L. Zhang, X. Lu, Q. Du *et al.*, “DeepSeek-Prover-V1.5: Harnessing Proof Assistant Feedback for Reinforcement Learning and Monte-Carlo Tree Search,” *arXiv preprint arXiv:2408.08152*, 2024.
- [17] R. Xin, C. Xi, J. Yang, F. Chen, H. Wu, X. Xiao, Y. Sun, S. Zheng, and M. Ding, “BFS-Prover: Scalable Best-First Tree Search for LLM-based Automatic Theorem Proving,” in *Proc. 63rd Annual Meeting of the Association for Computational Linguistics (ACL)*, vol. 1, 2025, pp. 32 588–32 599.
- [18] F. Gloeckle, J. Limperg, G. Synnaeve, and A. Hayat, “ABEL: Sample Efficient Online Reinforcement Learning for Neural Theorem Proving,” in *Proc. 4th Workshop on Mathematical Reasoning and AI at NeurIPS ’24*, 2024. [Online]. Available: <https://openreview.net/forum?id=kk3mSjVCUO>
- [19] K. Yang, A. M. Swope, A. Gu, R. Chalamala, P. Song, S. Yu, S. Godil, R. Prenger, and A. Anandkumar, “LeanDojo: Theorem Proving with Retrieval-Augmented Language Models,” in *Proc. 37th Conf. Neural Information Processing Systems (NeurIPS) Datasets and Benchmarks Track*, 2023. [Online]. Available: <https://openreview.net/forum?id=g7OX2sOJtn>
- [20] A. Q. Jiang, S. Welleck, J. P. Zhou, T. Lacroix, J. Liu, W. Li, M. Jamnik, G. Lampl, and Y. Wu, “Draft, Sketch, and Prove: Guiding Formal Theorem Provers with Informal Proofs,” in *Proc. 11th Int. Conf. Learning Representations (ICLR)*, 2023. [Online]. Available: <https://openreview.net/forum?id=SMa9EAovKMC>
- [21] X. Ji, Y. Liu, Q. Wang, J. Zhang, Y. Yue, R. Shi, C. Sun, F. Zhang, G. Zhou, and K. Gai, “Leanabell-Prover-V2: Verifier-integrated Reasoning for Formal Theorem Proving via Reinforcement Learning,” *arXiv preprint arXiv:2507.08649*, 2025.
- [22] Z. Ren, Z. Shao, J. Song, H. Xin, H. Wang, W. Zhao, L. Zhang, Z. Fu, Q. Zhu, D. Yang *et al.*, “DeepSeek-Prover-V2: Advancing Formal Mathematical Reasoning via Reinforcement Learning for Subgoal Decomposition,” *arXiv preprint arXiv:2504.21801*, 2025.
- [23] S. Rajase, K. Pratik, G. Cesa, and A. Behboodi, “Local Look-Ahead Guidance via Verifier-in-the-Loop for Automated Theorem Proving,” in *Proc. Workshop on Reasoning and Planning for Large Language Models (RapLLMs)*, 2025. [Online]. Available: <https://openreview.net/forum?id=e6VJwdnd8s>
- [24] C. Cao, L. Song, Z. Li, X. Le, X. Zhang, H. Xue, and F. Yang, “Reviving DSP for Advanced Theorem Proving in the Era of Reasoning Models,” *arXiv preprint arXiv:2506.11487*, 2025.
- [25] Y. Zhou, J. Zhao, Y. Zhang, B. Wang, S. Wang, L. Chen, J. Wang, H. Chen, A. Jie, X. Zhang *et al.*, “Solving Formal Math Problems by Decomposition and Iterative Reflection,” *arXiv preprint arXiv:2507.15225*, 2025.
- [26] D. Guo, D. Yang, H. Zhang, J. Song, P. Wang, Q. Zhu, R. Xu, R. Zhang, S. Ma, X. Bi *et al.*, “DeepSeek-R1 incentivizes reasoning in LLMs through reinforcement learning,” *Nature*, vol. 645, no. 8081, pp. 633–638, 2025.
- [27] A. Liu, B. Feng, B. Xue, B. Wang, B. Wu, C. Lu, C. Zhao, C. Deng, C. Zhang, C. Ruan *et al.*, “DeepSeek-V3 Technical Report,” *arXiv preprint arXiv:2412.19437*, 2024.
- [28] G. Comanici, E. Bieber, M. Schaeckermann, I. Pasupat, N. Sachdeva, I. Dhillon, M. Blistein, O. Ram, D. Zhang, E. Rosen *et al.*, “Gemini 2.5: Pushing the Frontier with Advanced Reasoning, Multimodality, Long Context, and Next Generation Agentic Capabilities,” *arXiv preprint arXiv:2507.06261*, 2025.

- [29] J. Schulman, F. Wolski, P. Dhariwal, A. Radford, and O. Klimov, “Proximal policy optimization algorithms,” *arXiv preprint arXiv:1707.06347*, 2017.
- [30] R. Rafailov, A. Sharma, E. Mitchell, C. D. Manning, S. Ermon, and C. Finn, “Direct Preference Optimization: Your Language Model is Secretly a Reward Model,” in *Proc. Advances in Neural Information Processing Systems (NeurIPS)*, vol. 36, 2023, pp. 53 728–53 741.
- [31] Q. Yu, Z. Zhang, R. Zhu, Y. Yuan, X. Zuo, Y. Yue, W. Dai, T. Fan, G. Liu, L. Liu *et al.*, “DAPO: An Open-Source LLM Reinforcement Learning System at Scale,” *arXiv preprint arXiv:2503.14476*, 2025.
- [32] A. W. He, D. Fried, and S. Welleck, “Rewarding the Unlikely: Lifting GRPO Beyond Distribution Sharpening,” in *Proc. 2025 Conf. Empirical Methods in Natural Language Processing (EMNLP)*, Suzhou, China, Nov. 2025, pp. 25 548–25 560.
- [33] Z. Peng, Y. Yao, K. Ma, S. Guo, Y. Li, Y. Zhang, C. Zhang, Y. Zhang, Z. Yu, L. Li, M. Liu, Y. Xia, J. Shen, Y. Wu, Y. Cao, Z. Zhang, W. Huang, J. Liu, and G. Zhang, “Criticlean: Critic-Guided Reinforcement Learning for Mathematical Formalization,” *arXiv preprint arXiv:2507.06181*, 2025.
- [34] Hugging Face, “Open R1: A Fully Open Reproduction of DeepSeek-R1,” Jan. 2025. [Online]. Available: <https://github.com/huggingface/open-r1>
- [35] J. Zhang and C. Zuo, “GRPO-LEAD: A Difficulty-Aware Reinforcement Learning Approach for Concise Mathematical Reasoning in Language Models,” *arXiv preprint arXiv:2504.09696*, 2025.